AAPG Annual Convention
Salt Lake City, Utah
May 11-14, 2003

Dating Groundwater Associated with Coalbed Methane Gas Wells in the San Juan Basin, USA

ZHENG ZHOU, Department of Earth Sciences, Swiss Federal Institute of Technology, Zurich, Switzerland; CHRIS J. BALLENTINE, Department of Earth Sciences, The University of Manchester, Manchester, UK; ROLF KIPFER, Swiss Federal Institute for Environmental Science and Technology, Zurich, Switzerland; MARTIN SCHOELL, GasConsult International L.L.C., Danville, CA; and STEVE THIBODEAUX, Burlington Resources, Farmington, NM.

Introduction

The role of groundwater in the generation of coalbed methane remains an open question. Some research shows that it provides the vector for microbial fertilization of isolated or previously sterilized subsurface environments (Scott et al., 1994; Martini et al., 1996; Tseng and Onstott, 1997;). Groundwater can interact with hydrocarbons, affecting the quality and commercial value of a hydrocarbon system by processes such as ''water washing'', and in other hydrocarbon systems plays a key role in pore creation and destruction (Lafargue and Barker, 1988; Aplin and Warren, 1994; Summa, 1995). Groundwater is also an important factor when assessing the usefulness of gas-depleted coalbeds for the long-term storage of anthropogenic CO_2. The amount of water, the hydrodynamic regime and water chemistry all play a role in the efficiency of CO_2 adsorption on the coal.

At present noble gases provide one of the best tools to quantify subsurface gas and water interaction (Ballentine et al., 1991; 1996; 2002; Ballentine and Sherwood Lollar, 2002). Noble gas isotopic composition and abundance can also be used to place constraints on fluid sources, their mass balance, phase interactions, and the mechanisms of transport required to bring the fluid to the site of sampling. The noble gases from the terrestrial atmosphere, can be distinguished isotopically from those produced by the decay of U, Th and K in the crust, and those derived from the mantle containing a primordial signature. Combined with the distinct elemental abundance patterns, it is possible to resolve the relative noble gas contribution from these different sources to any crustal fluid, and constrain the extent of crustal, mantle and atmosphere-derived noble gas involvement in these systems (Ballentine *et al.*, 2002; Ballentine and Burnard, 2002).

We show in this abstract how noble gases in the gas phase of producing coalbed methane gas wells in the San Juan Basin, USA, can be used to develop a physical model to describe gas/water interaction, to quantify the role of groundwater in coalbed systems and, for the first time, to obtain a ^4He age of the associated groundwater system.

Geological setting and sample locations

The San Juan Basin, one of the worlds largest commercial coalbed methane gas fields, is located on the eastern margin of the Colorado Plateau, USA (Fig. 1). Its structural evolution, maturity and coal rank, gas composition and isotope geochemisty are all well characterised (Kaiser et al., 1991; Scott et. al., 1994; Kaiser, 1998). This makes it a perfect environment to develop the noble gas tool to study the interaction between groundwater and subsurface hydrocarbons.

The coal was deposited as peats during Late Cretaceous. Localized post-coalification structural uplift occurred in the northernmost part of the basin, which caused a structural hingeline. In the north part of the hingeline, the coalbed is highly fractured with a high water permeability (up to a transmissivity of 130 ft^2 /d), but to the south of the hingeline the water permeability is low (down to a transmissivity of 0.6 ft^2/d).

Meteoric water recharges the coalbed on the northwest margin of the basin. To the north of the structural hingline, the aquifer is an artesian overpressured region, with the hingeline forming a barrier for the water flowing to the southern basin. To the south of the structrual hingeline, the aquifer is underpressured due to the low permeability.

25 natural gas samples were taken from producing wells in the San Juan Basin within the area enclosed by the dashed line in Fig. 1. Of these, 8 were control samples from the low production region south of the basin hingeline. The remaining samples are all from the hydrodynamically overpressured and high methane production region to the north.

Results and discussions
The results show that in both the underpressured and overpressured area, $^{3}He/^{4}He$ and $^{40}Ar/^{36}Ar$ ratios increase consistently according to the distance to the north-west basin margin (Fig. 2), indicating coherent noble gas behavior on a basin scale.

In addition, $^{3}He/^{4}He$ and $^{40}Ar/^{36}Ar$ ratios are all distinct from air ratios. Air contribution to He is negligible and variation in $^{3}He/^{4}He$ is caused by a two component mixture of magmatic and crustal-radiogenic He. A resolvable magmatic He component in all samples requires a deep crustal He flux from beneath the basin. $^{40}Ar/^{36}Ar$ ratios greater than air are due to a resolvable crustal-radiogenic $^{40}Ar^{*}$ component. ^{20}Ne and ^{36}Ar are derived from air dissolved in the groundwater at recharge. The isotopic ratios enable us to resolve the differently sourced noble gas components and, by looking at the fractionation of these components, identify the processes occurring between the gas and water phases.

Water derived noble gas $^{20}Ne/^{36}Ar$ ratios and radiogenic $^{4}He/^{40}Ar^{*}$ ratios in all samples show a clear fractionation trend (Fig. 3). This trend can be modelled as a Rayleigh fractionation of noble gases in the groundwater exsolving into the gas phase. Because the fractionation occurs in both water-derived noble gases and radiogenic noble gas pairs, it tells us that the radiogenic ^{4}He and $^{40}Ar^{*}$ are also dissolved in the groundwater before fractionation into the gas phase.

Nevertheless, a plot of ^{20}Ne concentrations versus $^{136}Xe/^{36}Ar$ (Fig. 4) shows that ^{20}Ne concentrations in samples are several orders of magnitude lower than the concentrations predicted by this model. This suggests that a component of the CH_4 has not equilibrated or ''seen'' groundwater at all. We have modelled this as methane gas desorbed from the coalbed, which in turn dilutes the ^{20}Ne concentrations in the groundwater equilibrated CH_4.

The samples we collected at the wellheads are a mixture of gas derived from groundwater and the dilution gas desorbed from the coalbed. Based on this model, we have calculated water gas volume ratios. From the available gas production history, we are able to achieve a primary objective and for the first time quantify the amount of groundwater associated with each production well. Fig. 5 shows the calculated water/gas production ratios against distance to basin margin recharge area.

It is clear that both in overpressured and underpressured regions, the gas wells close to the basin margin recharge area have seen significantly more water than gas wells towards the basin center. However, there is more water associated with per unit production of gas for the wells in the underpressured region than the gas wells in the overpressured region.

Calculating ^{4}He groundwater ages
Since radiogenic ^{4}He is dissolved into the groundwater before partitioning into the natural gas phase, it is possible to calculate the original ^{4}He concentration in the groundwater based on the Rayleigh fractionated water degassing model. The total original ^{4}He in the groundwater is in turn the sum of the *in situ* ^{4}He production and the *external* flux.

The *in situ* ^{4}He production has been estimated by taking U and Th coalbed concentrations of 1.5ppm and 4.6ppm respectively. The ^{4}He accumulation rate in the aquifer is a function of the pores occupied by the water, which are 23% for the overpressured region and 3% for the underpressured region. This gives an *in situ* production rate of 2.38×10^{-12} and 1.82×10^{-11} ccSTP$^{4}He/ccH_2O.yr$ for the overpressured and underpressured area respectively.

The accumulation rate is also a function of the *external* crustal ^{4}He flux, the aquifer porosity and the thickness of the aquifer. For our preliminary calculations we have assumed an average crustal ^{4}He flux of 2.31×10^{-6} ccSTP $^{4}He/cm^{2}.yr$ to give an *external* ^{4}He accumulation rate of 3.35×10^{-10} and 2.57×10^{-9} ccSTP$^{4}He/ccH_2O.yr$ for the overpressured and underpressured area respectively. The ^{4}He groundwater dates for San Juan samples are therefore directly proportional to the calculated original ^{4}He groundwater concentration, and are dominated by the external ^{4}He flux. Full equations and discussions can be found in Torgerson and Clarke, 1985 and Ballentine et. al., 2002.

Fig. 6 shows the preliminary ^{4}He dates of the groundwater associated with each of the San Juan Basin coalbed gases. The dates in the overpressured region range from 1.9×10^{3} to 1.0×10^{5} years. The dates in the underpressured region range from 7.2×10^{3} to 3.9×10^{4} years. However, both in the overpressured and underpressured region, groundwater ages are dominated by samples with an age of less than 10,000 years.

The dominant uncertainty used to derive the groundwater ^{4}He dates is in the assumption of an average crustal *external* ^{4}He flux into the aquifer system. Although the absolute dates are currently subject to significant uncertainty, the relative ^{4}He dates obtained will be reasonable. Current work is underway to better constrain the ^{4}He flux estimates used in our preliminary calculations.

Conclusions

Both water-derived and radiogenic noble gases in the San Juan Basin natural gas reservoir follows a simple Rayleigh fractionation model. Low ^{20}Ne concentrations in gas samples can be accounted for by dilution of the groundwater associated gas by desorbed coalbed methane. This model allows us to quantify the amount of water associated with each well. The results show that the gas wells close to the basin margin recharge area have seen significantly more water, relative to the amount of gas produced, than gas wells towards the basin center. However, there is more water associated with per unit production of gas for the wells in the underpressured region than gas wells in the overpressured region. The ^{4}He groundwater ages across the high production region, assuming an average crustal ^{4}He flux, is consistent with groundwater that was recharged 2,000-5,000 years ago, and on average is significantly younger than the ^{4}He groundwater age of the low production/underpressured portion of the basin.

References

Aplin A. C. and Warren E. A., 1994. Oxygen indications of the mechanism of silica transport and quartz cementation in deeply buried sandstones. Geology 22, 847-850.

Ballentine C. J., O'Nions R. K., Oxburgh E. R., Horvath F., and Deak J., 1991. Rare gas constraints on hydrocarbon accumulation, crustal degassing and groundwater flow in the Pannonian Basin. Earth and Planetary Science Letters 105, 229-246.

Ballentine C. J., O'Nions R. K., and Coleman M. L., 1996. A Magnus opus: He, Ne and Ar isotopes in a North Sea oil field. Geochimica et Cosmochimica Acta 60, 831-849.

Ballentine C. J. and Sherwood Lollar B., 2002. Regional groundwater focusing of nitrogen and noble gases into the Hugoton-Panhandle giant gas field, USA. Geochimica et Cosmochimica Acta, Vol. 66, No. 14, 2483-2497.

Ballentine C. J., and Burnard P. G., 2002. Production, Release and Transport of Noble Gases in the Continental Crust. In Noble gases in geochemistry and cosmochemistry, Reviews in mineralogy and geochemistry (Editors: D. Porcelli, C. J. Ballentine and R. Wieler.). Vol. 47, 481-538.

Ballentine C. J., R. Burgess and B. Marty, 2002. Tracing Fluid Origin, Transport and Interaction in the Crust. In Noble gases in geochemistry and cosmochemistry, Reviews in mineralogy and geochemistry (Editors: D. Porcelli, C. J. Ballentine and R. Wieler.). Vol. 47, 539-614.

Kaiser, W. R., Ayers, W. B. Jr., Ambrose, W. A., Laubach, S. E., Scott, A. R., and Tremain, C. M., 1991. Geologic and hydrologic characterization of coalbed methane production, Fruitland Formation, San Juan Basin, in Ayers, W. B., Jr., et al., Geologic and hydrologic controls on the occurrence and producibility of coalbed methane, Fruitland Formation, San Juan Basin: Chicago, Gas Research Institute Topical Report GRI-91/0072, 273-301.

Kaiser, W. R., T. E. Swartz, and G. J. Hawkins, 1991. Hydrology of the Fruitland Formation, San Juan basin, in W. B. Ayers,

Jr., et al., Geologic and hydrologic controls of the occurrence and producibility of coalbed methane. Fruitland Formation, San Juan basin: Gas Research Institute Topical Report GRI-91/0072, 195-241.

Kaiser, W. R., 1998. Hydrogeology of Coalbed Reservoirs. International Conference on Coal-Seam Gas and Oil, 423-472.

Lafargue E. and Barker C., 1988. Effect of water washing on crude-oil compositions. AAPG Bull. 72, 263-276.

Martini A. M., Budai J. M., Walter L. M., and Schoell M., 1996. Microbial generation of economic accumulations of methane within a shallow organic-rich shale. Nature 383, 155-158.

Scott A. R., Kaiser W. R., and Walter Jr. B. A., 1994. Thermogenic and secondary biogenic gases, San Juan basin, Colorado and New Mexico - Implications for coalbed gas producibility. AAPG Bull 8, 1186-1209.

Summa L. L., 1995. Diagenesis and reservoir quality prediction. Review of Geophysics 33, 87-94.

Torgerson T. and W. B. Clarke, 1985. Helium accumulation in groundwater, I: An evaluation of sources and the continental flux of crustal ^{4}He in the Great Artesian Basin, Australia, Geochimica et Cosmochimica Acta Vol. 49, 1211-1218.

Tseng H. Y. and Onstott T. C., 1997. A tectonic origin for the deep subsurface microorganisms of Taylorsville Basin: Thermal and fluid flow model constraints. FEMS Microbiol. Rev. 20, 391-397.

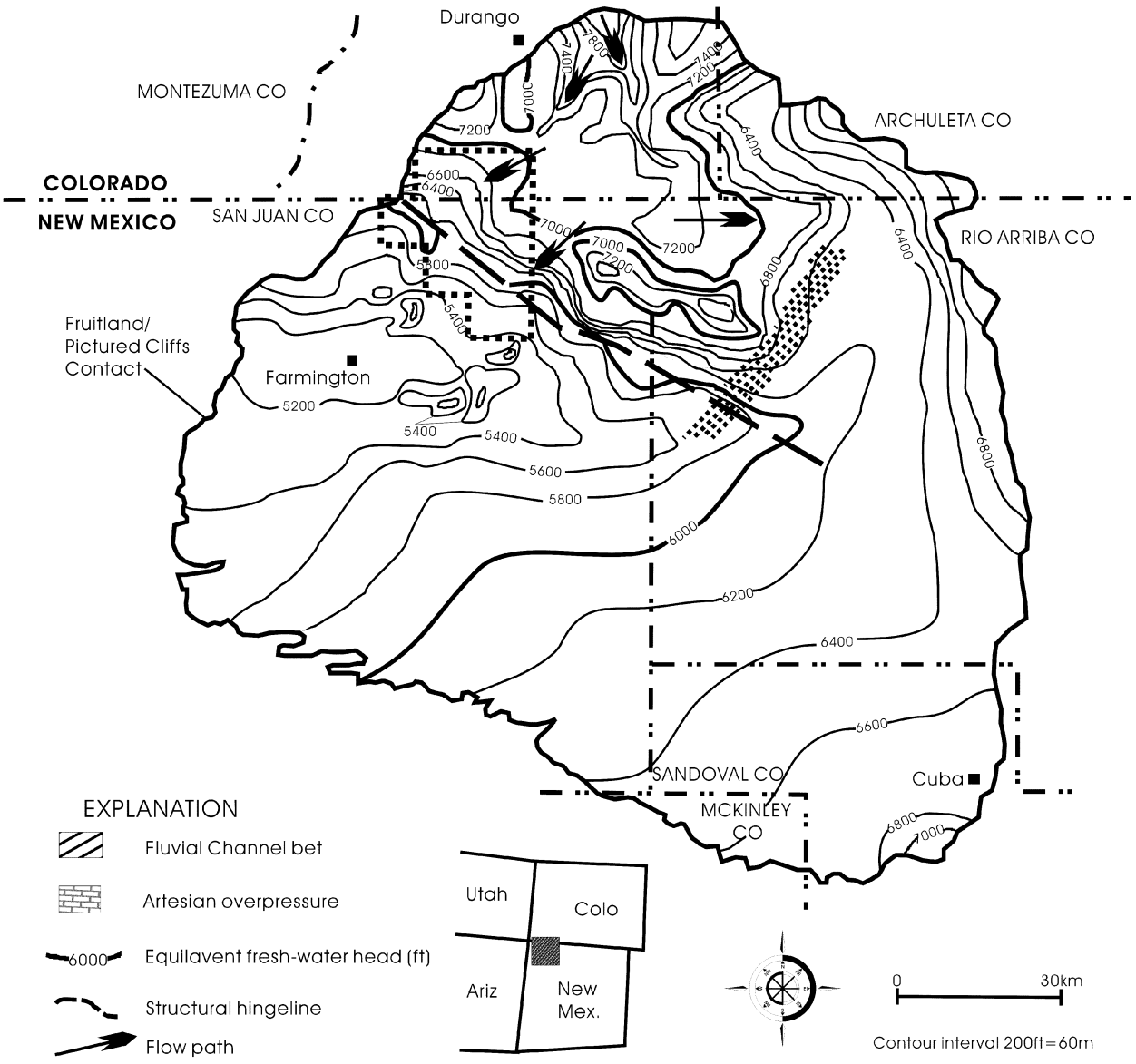

Fig. 1 Geological setting of the San Juan Basin and sampling area (after Scott et. al., 1994)

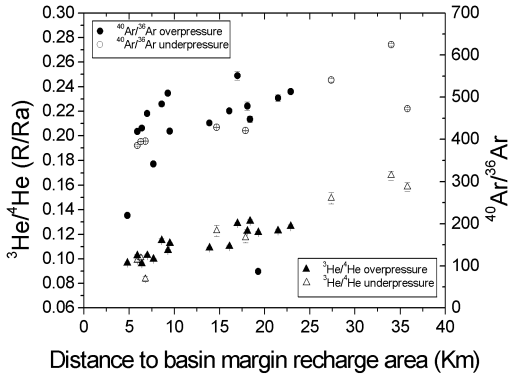

Fig. 2 Coherent $^{3}He/^{4}He$ and $^{40}Ar/^{36}Ar$ trend

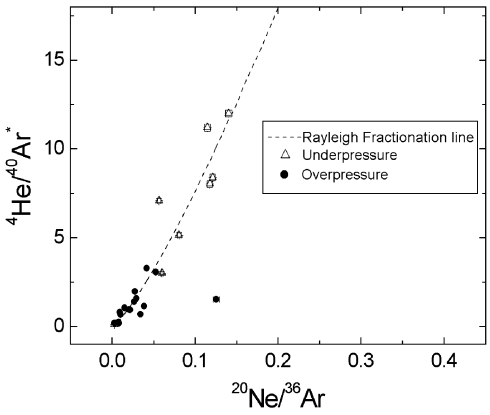

Fig. 3 Water-derived $^{20}Ne/^{36}Ar$ vs. Radiogenic $^{4}He/^{40}Ar^{*}$

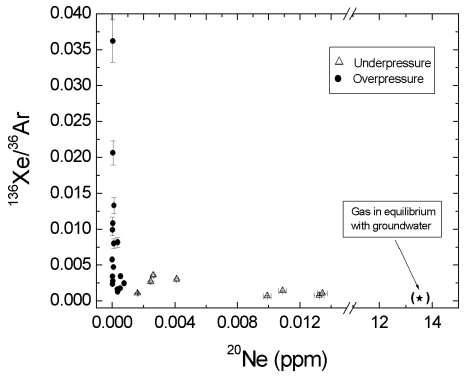

Fig. 4 ^{20}Ne Concentration vs. $^{136}Xe/^{36}Ar$

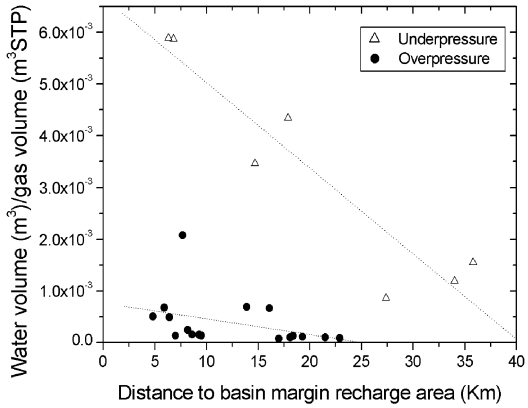

Fig. 5 Calculated water/gas production ratio vs. distance to basin margin recharge area

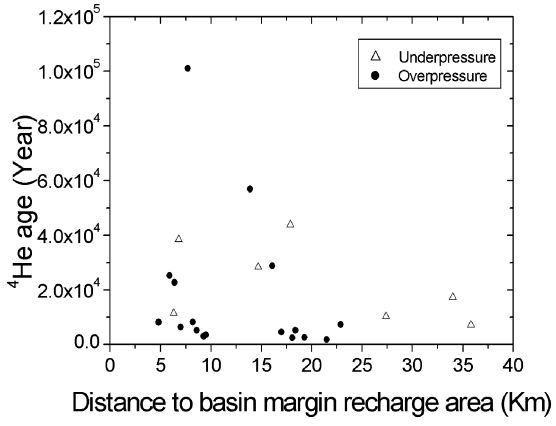

Fig. 6 ^{4}He dating of groundwater, San Juan Basin